

See discussions, stats, and author profiles for this publication at: <https://www.researchgate.net/publication/235639253>

Pressureless reaction sintering of yttrium aluminium garnet (YAG) from powder precursor in the hydroxyhydrogel form

ARTICLE *in* CERAMICS INTERNATIONAL · DECEMBER 2011

Impact Factor: 2.61 · DOI: 10.1016/j.ceramint.2011.04.137

CITATIONS

3

READS

44

4 AUTHORS, INCLUDING:



[Sunipa Bhattacharyya](#)

National Institute of Technology Rourkela

10 PUBLICATIONS 38 CITATIONS

SEE PROFILE



[Kausik Dana](#)

Council of Scientific and Industrial Research...

39 PUBLICATIONS 362 CITATIONS

SEE PROFILE



Pressureless reaction sintering of yttrium aluminium garnet (YAG) from powder precursor in the hydroxyhydrogel form

Sunipa Bhattacharyya, T.K. Mukhopadhyay, Kausik Dana, Sankar Ghatak *

Central Glass and Ceramic Research Institute, CSIR, Advanced Clay and Traditional Ceramic Division, 196, Raja S.C. Mullick Road, Kolkata 700032, India

Received 16 November 2010; received in revised form 14 February 2011; accepted 26 April 2011

Abstract

Pressureless reaction sintering of YAG was carried out by using a precursor powder in the hydroxyhydrogel form synthesized by flash polycondensation technique. Reactive silica additive was used to modify Al–O–Y network where Si^{4+} was incorporated in the solvated form. The sintering experiments were carried out with the processed powder up to 1650 °C under ambient ambience. Densification indicated effective sintering with well-formed microstructure. Phase identification by XRD indicated only YAG in the sintered specimen.

© 2011 Elsevier Ltd and Techna Group S.r.l. All rights reserved.

Keywords: Fumed silica; Solvation layer; Sintering additive; YAG

1. Introduction

In recent years, among the garnet structure oxides, yttrium aluminium garnet (YAG) has become popular as high temperature engineering material due to its high temperature strength coupled with low creep rate. It has high melting temperature (1940 °C) high stability in both oxidising and reducing atmosphere. Its coefficient of thermal expansion is low making it a good match for many potential oxide matrices. Its excellent creep properties and oxidative stability make it a candidate for high temperature engine component [1]. However, sintering of YAG makes a problem due to low volume diffusivity and tendency of phase change of YAG to alumina rich or yttria rich composition depending on processing condition. This problem necessitated use of sintering additive such as magnesium oxide, silica etc. Sintering of YAG by using silica as an additive was done either by incorporating silica as an oxide or tetra ethyl orthosilicate. Sintering operation is normally carried out under vacuum or in hydrogen atmosphere at 1700 °C. Regarding the role of silica there are different opinions. For example, Vrolijk et al. [2] suggested an increase of grain boundary diffusion co-efficient or a decrease of grain boundary energy due to the

occurrence of secondary phases for sintering of YAG in presence of SiO_2 . On the other hand, Wang et al. [3] suggested that silica phase may influence a solid solution formation by replacing Al^{3+} by Si^{4+} in tetrahedral site of YAG. This transformation may lead to the formation of Al^{3+} vacancies which would enhance the lattice diffusion co-efficient and as a result YAG densification kinetics will improve. It is further claimed [4] that silica addition leads to the formation of several phases, composition of which varies with sintering temperature. In some cases this lead to the fusible phases. Formation of liquid phase which appears at around 1387 °C would result from the solid–solid reaction between silica and YAG particles. The chemical composition of the liquid phase so formed was reported to be belonging to the eutectic compound in SiO_2 – Al_2O_3 – SiO_2 ternary diagram [5–7]. It is also observed that the densification rate of YAG increased with increasing the amount of silica may be due decreased fractional solid–solid contact area and the enhancement of kinetic mass transport by diffusion through the liquid phase [8].

As the amount of sintering additive is very low for homogeneous densification, a uniform distribution of silica in the bulk is also essential. It is obvious that homogeneous mixing of silica (solid) as such is difficult to achieve. Alternatively [9–11] tetra ethyl orthosilicate is tried. It was found that double mixing treatment first in ethanol then in water, promotes the hydrolysis of tetra ethyl orthosilicate and its homogeneous distribution on to the oxide particle surface

* Corresponding author. Tel.: +91 33 2429 4180; fax: +91 33 2473 0957.

E-mail address: sghatak@cgcricri.res.in (S. Ghatak).

[10]. It is also known that the direct mixing in water inhibits the tetra ethyl orthosilicate hydrolysis. Tetra ethyl orthosilicate has another disadvantage of decomposition with a chance of leaving carbon in the system.

In all the previous sintering experiments, [9–11] vacuum sintering at higher temperature was adopted for developing transparency in the sintered compact for optical use. However, for engineering applications transparency is not a necessary property and the cost of sintering may be reduced if pressureless sintering is adopted for sintering of YAG ceramic. The objective of the present work was concentrate on homogeneous distribution of sintering additive and study sintering under normal pressure.

2. Experimental

Four batches of precursor powder were prepared by maintaining $Y_2O_3:Al_2O_3$ ratio equal to 3:5 and varying fumed silica content in the range 0–2.5%. The yttrium and aluminium sources for synthesis of powder precursor were 99.9% $Y(NO_3)_3 \cdot 6H_2O$ (Aldrich) and 99.9% $Al(NO_3)_3 \cdot 9H_2O$ (Merck). As precipitant, 25% ammonia water was used (analytical grade). Saturated solution of yttrium nitrate and aluminium nitrate were prepared in distilled water. Required amount of solution of yttrium nitrate and aluminium nitrate were mixed in such a proportion that ultimately the powder maintains $Y_2O_3:Al_2O_3$ at 3:5 molar ratios. Fumed silica (Cab-o-Sil) in required amount (Table 1) is mixed to provide silica content at 0%, 0.5%, 1.5%, and 2.5% of the total solids in the final product. The mixed solution was stirred vigorously for 2 h for complete homogenisation. This mixed material was polymerised by “flash polycondensation technique” [12–17] to obtain a gel-like mass, which was kept for 24 h without stirring. The extraneous soluble impurities were removed by washing with hot water and the solid mass left was dried at $110 \pm 10^\circ C$. The dried materials were characterised by DTA-TG. A small amount of powder was heat treated at temperatures from $700^\circ C$ to $1200^\circ C$ for ascertaining the formation of desired phase. Powder was calcined at $830^\circ C$ and ground in an agate mortar and passed through 300 mesh sieves. These materials were used to fabricate discs of dimension 25 mm diameter and 5 mm thickness under uniaxial pressing followed by isostatic pressing under 250 MPa. Discs were sintered at $1400^\circ C$ to $1650^\circ C$ in electrically heated furnace in normal atmosphere. Densification of the sintered compacts was studied by measuring linear shrinkage, bulk density and apparent porosity of the samples.

Table 1
Batch composition: (Basis: 100 gm of uncalcined dried powder).

Sample no.	Yttrium nitrate solution ^a (ml)	Aluminium nitrate solution ^b (ml)	Fumed silica (g)
1	256	744	0 (0%)
1A	256	744	0.5 (0.5%)
1B	256	744	1.5 (1.5%)
1C	256	744	2.5 (2.5%)

^a0.162 g Y_2O_3 /ml.

^b0.042 g Al_2O_3 /ml.

Phase and microstructure evolution was studied using XRD and electron microscopy respectively. Thermal analysis of precursor powder was done using NETZSCH Thermal analyzer STA409 instrument up to $1000^\circ C$ at a heating rate of $10^\circ C$ /min. Phase analysis was carried out by X-ray diffractometer (PW 1730, Phillips, (Holland). Microstructures were studied by using a scanning electron microscope (LEO 430i, LEO UK).

3. Results and discussion

Fig. 1 shows the variation of linear shrinkage with sintering temperature of powder compacts in the $Y_2O_3-Al_2O_3$ system containing different amount of fumed silica additive. Percent linear shrinkage was found to increase linearly with increasing heat treatment temperature up to $1600^\circ C$ for all the batches containing different percent of silica. A sharp increase in shrinkage values was found at the temperature range of 1600 – $1650^\circ C$ for batch 1 to 1C. The slope of the curves in this temperature zone for batches 1 to 1C was given in Table 2. The values of the slopes indicated that the percent change in shrinkage with temperature in between $1600^\circ C$ and $1650^\circ C$ increased with increasing silica content from 0% to 2.5%.

Fig. 2 shows the change of percent apparent porosity of powder compacts containing different percent of fumed silica additive with increasing heat treatment temperature. Percent apparent porosity was found to decrease with increasing sintering temperature more or less uniformly up to $1600^\circ C$ beyond which a sharp fall was noted. From the slope of the curves in the temperature range 1600 – $1650^\circ C$ (Table 2) for different batches it was found that the percent change in apparent porosity increases with increasing silica content from 0% to 2.5%.

Fig. 3 shows the bulk density of powder compacts sintered at $1400^\circ C$ to $1650^\circ C$ in presence of different percent of fumed silica additive. It was found that bulk density gradually increases with increasing heat treatment temperature up to $1600^\circ C$ for all the batches containing different percent of silica additive, but beyond $1600^\circ C$, the increase in bulk density value was much sharper and this behaviour was common for all the batches. Slope measurement of bulk density temperature curve

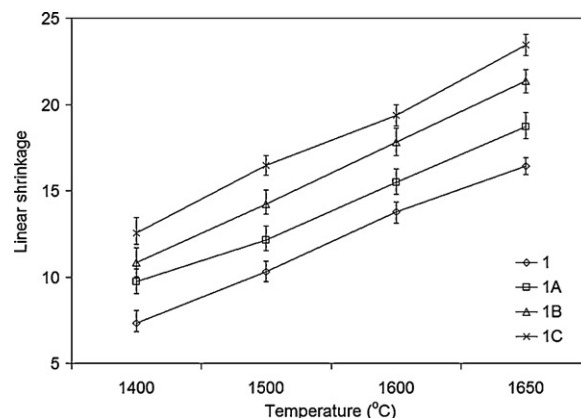


Fig. 1. Variation of shrinkage with heat treatment temperature for different percentage of silica additive.

Table 2

Slope of the curves at the temperature range 1600–1650 °C.

Type of the curve	Slope for batch-1	Slope for batch-1A	Slope for batch-1B	Slope for batch-1C
Shrinkage	0.053	0.065	0.081	0.081
Apparent porosity	0.070	0.073	0.077	0.086
Bulk density	0.0036	0.0036	0.0038	0.0042

beyond 1600 °C for batch 1 to 1C shows higher densification for higher percent of fumed silica additive.

In the present system, active Y^{3+} , Al^{3+} , O^{2-} and Si^{4+} remains to react with each other during heat treatment. SiO_2 may react with both Al_2O_3 and Y_2O_3 forming respective silicates, which is not desirable as formation of stoichiometric YAG is preferred. In view of the above, we attempted to generate such an intermediate phase which will preferentially form YAG keeping SiO_2 separated and is not allowed to react with either Y_2O_3 or Al_2O_3 . Here fumed silica was used as the source of silica. It is fairly well established [18,19] that fumed silica forms stable sols in liquids which possess sufficient capacity to form H-bonds. In the present system, i.e., in aqueous medium, liquid molecules organize at the silica interface by forming H-bonds with silanol ($Si-OH$) groups present on the silica surface. This would lead to a solvation layer that coats each silica unit. The strong binding of the liquid molecules within the solvation layer is then expected to contribute a short-range repulsive force preventing particle contact (Fig. 4). Thus, we can envision that the solvated particles are stabilized against coagulation by an additional repulsive force (“solvation force”) and that helps in uniform distribution of this additive in the mixed salt solutions.

The mixed salt solutions containing fumed silica when comes in contact with ammonium hydroxide polymerization takes place with the formation of polynuclear complex which consist of a network of Al^{3+} and Y^{3+} bonded by hydro, hydroxy and oxo bonds of different energies and Si^{4+} coated with a layer of water molecules distributed within the structure. Here yttrium ion is coordinated by four hydroxyl groups and four water molecules with the coordination number eight [20]. After

polymerisation the structure may assume either Fig. 5a or b. The difference between Fig. 5a and b is the position of solvated Si^{4+} in the structure. In all likelihood Si^{4+} will replace tetra coordinated aluminium and will go into network structure, the ultimate structure expected to be consisting of Al, Y, O and Si in the network. This assumes that after formation of YAG, Si^{4+} will remain in the structure where some of the Al^{3+} (tetrahedral) is replaced by Si^{4+} making the structure defective, but due to very small contribution of this phenomenon, it was not reflected in the XRD (Fig. 6).

From the results of sintering experiments, it appears that sintering is more or less uniform up to 1600 °C and degree of sintering increases with increasing silica content. Rapid sintering above 1600 °C was also noted up to 2.5% silica additive.

SEM analysis was conducted on all the samples fired at 1650 °C. Microstructure of specimen without containing any fumed silica additive (Fig. 7) indicates retention of grain with limited sintering and substantial pores (~14%). When small amount of silica 0.5% was used as additive (Fig. 8) the sintered samples indicate isolated grain growth with considerable porosity (12%). When the silica increased to 1.5% (Fig. 9) sintering was more with less porosity (9%), with 2.5% silica content (Fig. 10) rounding of grains were indicated, with minimum porosity about 5%.

In all earlier investigations [4,5,8,11,9] liquid phase were detected during sintering, where oxide raw materials were used and silica was added separately. In this case liquid phase sintering was proposed as densification mechanism. They also proposed that at higher sintering temperature the liquids disappear due to vaporisation of silica-rich secondary phase, particularly under low oxygen partial pressure. In the present

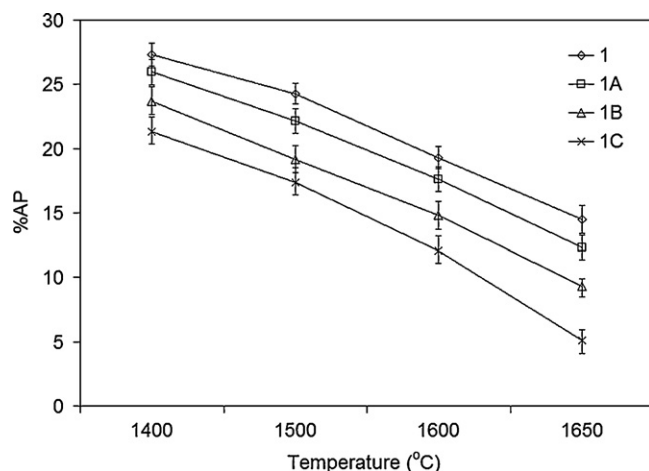


Fig. 2. Variation of %AP with increasing heat treatment temperature for different percentage of silica additive.

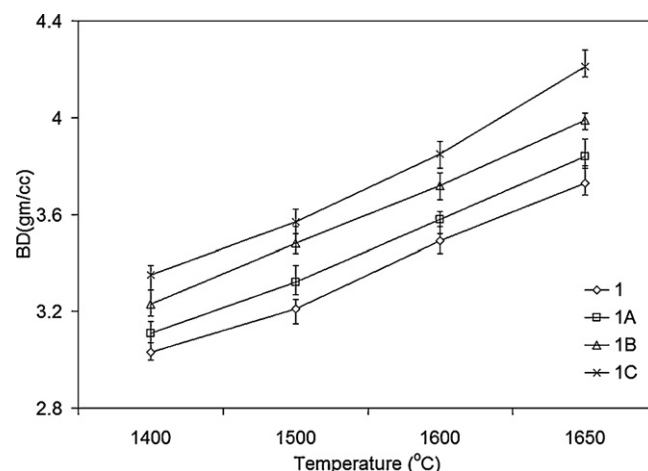


Fig. 3. Variation of BD with increasing heat treatment temperature for different percentage of silica additive.

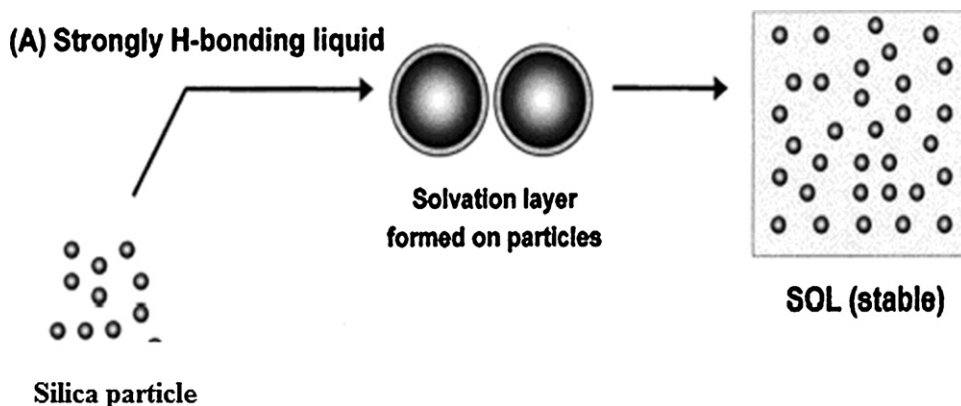


Fig. 4. Formation of solvated silica particle.

investigation, the sintering was conducted under normal atmospheric pressure in air, eliminating the condition generated due to low-pressure condition. Even under this condition no liquid phase could be detected in the microstructure.

The other possibility remains is the volume diffusivity which is enhanced by the substitution of Al^{3+} by Si^{4+} in tetrahedral site

of the crystallographic structure as follows: $3\text{SiO}_2 \xrightarrow{2\text{Al}_2\text{O}_3} 3\text{Si}_{\text{Al}}^0 + \text{V}_{\text{Al}}''' + 6\text{O}_0^x$

Though the solubility of Si^{4+} in YAG is low [3] when the powder precursor was prepared by wet chemical interaction the solubility limit is exceeded and larger amount of Si^{4+} may replace Al^{3+} in tetrahedral site. The possibility of substitution

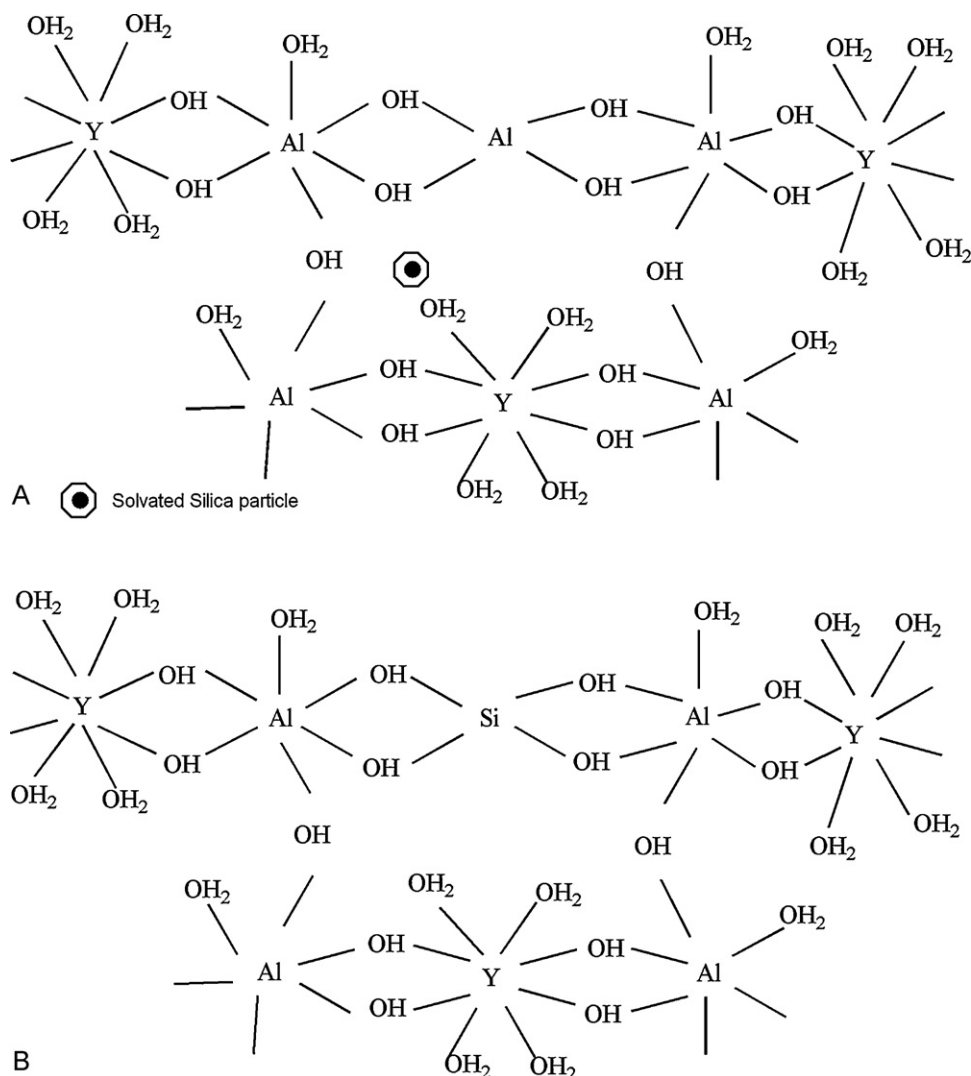


Fig. 5. (a) Imaginary structure of the polynuclear complex. (b) Imaginary structure of the polynuclear complex after substitution.

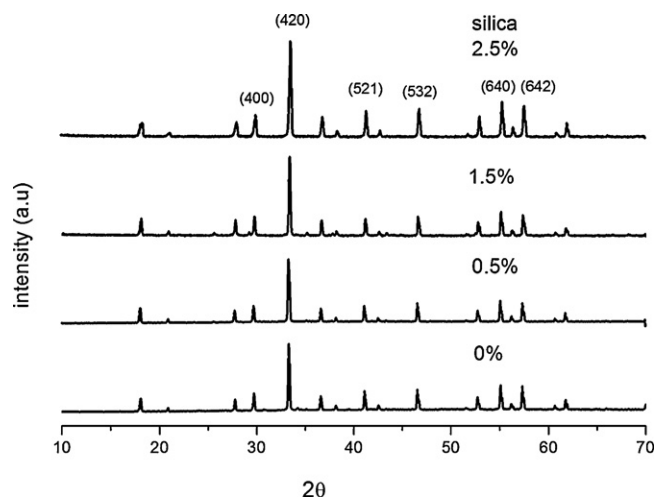


Fig. 6. X-Ray diffraction study of 1650 °C sintered samples (JCPDF file no-330040).

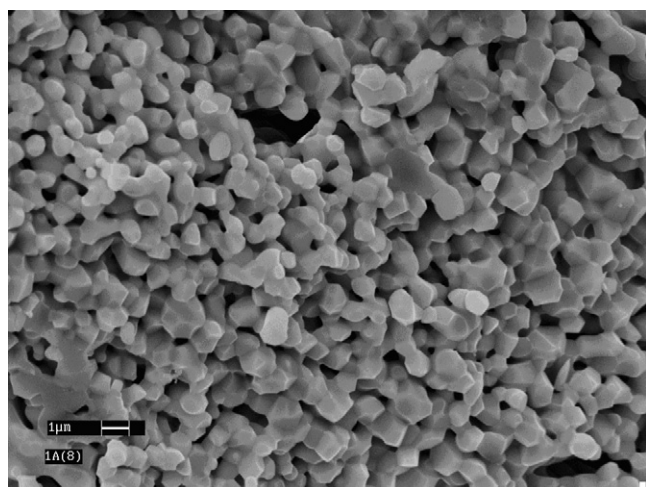


Fig. 7. SEM micrograph of Fracture surface of sample-1 (without additive).

of Al^{+3} by Si^{+4} can also be proved through indirect evidences. Kolitsch et al. [7] observed while studying the crystal chemistry in the $\text{Y}_2\text{O}_3\text{--Al}_2\text{O}_3\text{--SiO}_2$ system that there was a decrease of the lattice parameters a , b , c and of the cell volume with

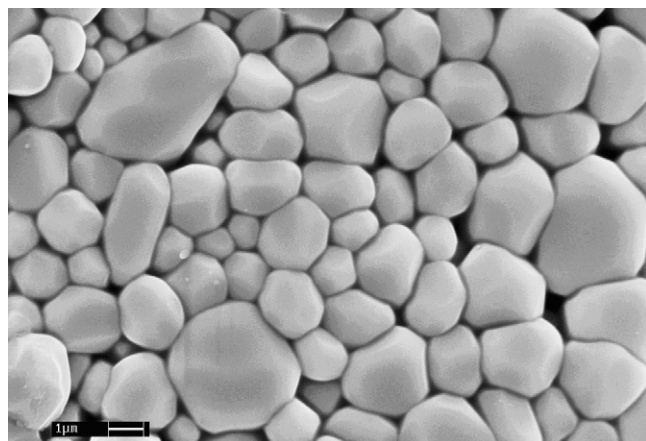


Fig. 8. SEM micrograph of Fracture surface of sample-1A (0.5% silica additive).

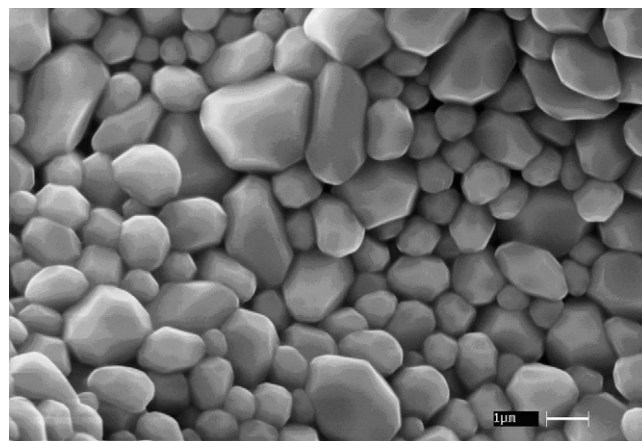


Fig. 9. SEM micrograph of Fracture surface of sample-1B (1.5% silica additive).

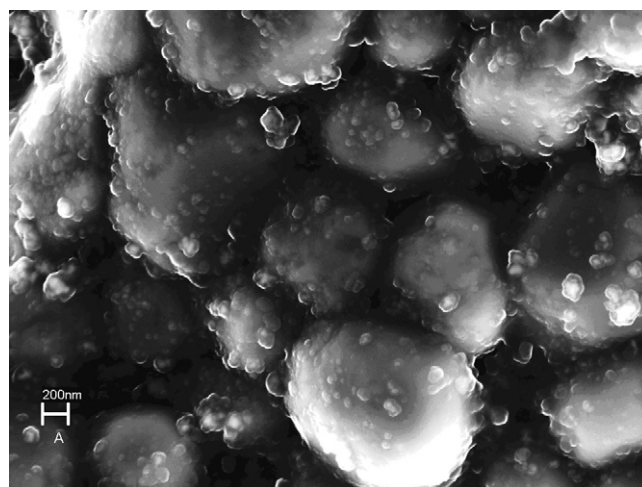


Fig. 10. SEM micrograph of polished surface of sample-1C (2.5% silica additive).

increasing silica content. The result is quite expected due to substitution of Al^{+3} with smaller sized Si^{+4} . Further, the increase of monoclinic angle β was explained by the shortening of the distance between two Al^{+3} ions in the YAG crystal structure when they were replaced by Si^{+4} ions, since these two ions are located almost within the (0 1 0) plane [21].

In all previous experiments silica was used in limited amount. In the present investigation, larger amount of silica was used and the effect of the silica when incorporated in the structure was more prominent. The incorporation of Si^{+4} in the YAG structure replacing Al^{3+} in the tetrahedral sites will thus leave some unutilised alumina in the system and the proportion of alumina will increase with increasing silica addition. In the microstructure of YAG with 2.5% SiO_2 at 1650 °C some precipitation of alumina was observed. These observations confirm the proposition of Si^{+4} replacing Al^{+3} leaving unutilised Al_2O_3 in the system.

4. Conclusion

This work emphasizes the role of silica on the densification behaviour of YAG. Effect of silica on the densification of YAG

studied by using fumed silica as an additive resulted into a more homogeneous and reactive intermediate. The precursor powder of YAG produced by wet chemical interaction sintered to a theoretical density of around 93% at 1650 °C in presence of 2.5% fumed silica additive. Here silica phase promote solid solution formation by replacing Al^{3+} by Si^{4+} in tetrahedral site of YAG. This transformation leads to the formation of Al^{3+} vacancies which would enhance the lattice diffusion co-efficient and helped to improve YAG densification kinetics.

Acknowledgements

The work was supported by CSIR fellowship grant to Mrs. Sunipa Bhattacharyya (currently working as senior research fellow in C.G.C.R.I, Kolkata) and is also included as a part of the network project CMM-0022. Authors are grateful to the Glass Science section, XRD section and SEM section for their constant support.

References

- [1] G.S. Corman, Creep of yttrium aluminium garnet single crystals, *J. Mater. Sci. Lett.* 12 (1993) 379–382.
- [2] J.W. Vrolijk, S. Van Dem Cruisem, R. Metselaar, The influence of MgO and SiO_2 dopants on the sintering behaviour of yttrium aluminium garnet ceramics, *Ceram. Trans.* 51 (1995) 573–577.
- [3] Y. Wang, L. Zhang, Y. Fan, J. Luo, D.E. McCready, C. Wang, L. An, Synthesis characterisation and optical properties of pristine and doped yttrium aluminium garnet nanopowder, *J. Am. Ceram. Soc.* 88 (2005) 284–286.
- [4] C. Salle, A. Maitre, J.F. Baumard, Y. Rabinovitch, A first approach of silica effect on the sintering of Nd:YAG, *Opt. Rev.* 14 (2007) 169–172.
- [5] A. Maitre, C. Salle, R. Boulesteix, J.-F. Baumard, Y. Rabinovitch, Effect of silica on the reactive sintering of polycrystalline Nd:YAG ceramics, *J. Am. Ceram. Soc.* 91 (2) (2008) 406–413.
- [6] A. Bondar, F.Ya. Glakhov, Phase equilibria in the system $\text{Y}_2\text{O}_3\text{--Al}_2\text{O}_3\text{--SiO}_2$, *Izv. Akad. Nauk SSSR Ser. Khim.* 7 (1964) 1325–1326.
- [7] U. Kolitsch, H.J. Seifert, T. Ludwig, F. Aldinger, Phase equilibria and crystal chemistry in the $\text{Y}_2\text{O}_3\text{--Al}_2\text{O}_3\text{--SiO}_2$ system, *J. Mater. Res.* 14 (2) (1999) 447–455.
- [8] R. Boulesteix, A. Maitre, J.-F. Baumard, C. Salle, Y. Rabinovitch, Mechanism of liquid phase sintering for Nd–YAG ceramics, *Opt. Mater.* 31 (2009) 711–715.
- [9] S. Kochawattana, A. Stevenson, S.-H. Lee, M. Ramirez, V. Gopalan, J. Dumm, V.K. Castillo, G.J. Quarles, G.L. Messing, Sintering and grain growth in SiO_2 doped Nd:YAG, *J. Eur. Ceram. Soc.* 28 (2008) 1527–1534.
- [10] L. Esposito, A. Luisa Costa, V. Medri, Reactive sintering of YAG based materials using micrometer sized powders, *J. Eur. Ceram. Soc.* 28 (2008) 1065–1071.
- [11] L. Wen, X. Sun, Z. Xiu, S. Chen, C.-T. Tasi, Synthesis of nanocrystalline yttria powder and fabrication of transparent ceramics, *J. Eur. Ceram. Soc.* 24 (2004) 2681–2688.
- [12] S. Ghatak, D. Basu, A.K. Samanta, H.S. Maiti patent no. 226626, 22.12.2008, India.
- [13] S. Bhattacharyya, S. Ghatak, Synthesis and characterization of YAG precursor powder in the hydroxyhydrogel form, *Ceram. Int.* 35 (2009) 29–34.
- [14] A.K. Basu, A. Mitra, S. Ghatak, Synthesis of a powder precursor in the form of hydroxyhydrogel for reaction sintering of BN–mullite composite, *Ceram. Int.* 32 (2) (2000) 213–219.
- [15] S. Mandal, S. Chakrabarti, S. Ghatak, Preparation and characterization of a powder precursor, consisting of oxides of Li–Al–Si in the form of hydroxyhydrogel for synthesis of β -spodumene, *Ceram. Int.* 30 (3) (2004) 357–367.
- [16] S. Mandal, S. Chakrabarti, S. Das, S. Ghatak, Sintering characteristics of in situ formed low expansion ceramics from a powder precursor in the form of hydroxyhydrogel, *Ceram. Int.* 30 (8) (2004) 2147–2155.
- [17] A.K. Samanta, K.K. Dhargupta, A.K. De, S. Ghatak, SiC–YAG sintered composites from hydroxy hydrogel powder precursors, *Ceram. Int.* 26 (8) (2000) 831–838.
- [18] M.Q. Chen, H.Y. Chen, D. Shu, A.J. Li, D.E. Finlow, Effects of preparation condition and particle size distribution on fumed silica gel valve-regulated lead acid batteries performance, *J. Power Sources* 181 (2008) 161–171.
- [19] S.R. Raghavan, H.J. Walls, S.A. Khan, Rheology of silica dispersion in organic liquids: new evidence for solvation forces dictated by hydrogen bonding, *Langmuir* 16 (2000) 7920–7930.
- [20] F. Gao, R.-Y. Wang, T.-Z. Zin, G.-X. Xu, Z.-Y. Zhou, X.-G. Zhou, Synthesis and crystal structure of a heteronuclear copper and yttrium complex with alanine $[\text{CuY}(\text{Ala})_4(\text{H}_2\text{O})_5](\text{ClO}_4)_5 \cdot 3\text{H}_2\text{O}$, *Polyhedron* 16 (8) (1997) 1357–1360.
- [21] A.N. Christensen, R.G. Hazell, A comparison of three sets of diffraction data for $\text{Al}_2\text{Y}_4\text{O}_9$: X-ray synchrotron powder data, X-Ray single crystal data from Ag $\text{K}\alpha$ radiation, and neutron single crystal data from 1.01 Å neutrons, *Acta Chem. Scand.* 45 (1991) 226–230.